Roll Metrics for Handling Qualities: The Landing Approach

Ajay Thukral* and Mario Innocenti†
Auburn University, Auburn, Alabama 36849

Introduction

HIGHLY augmented aircraft have shown handling qualities degradation in the roll axis due to increased flight control system augmentation and high-order effects.[1] In a recent paper,[2] alternate metrics were proposed, based on Gibson's method, to identify handling qualities deficiencies, and level 1 boundaries were established for the tracking task.

In the present paper, new guidelines for the landing task are presented and validated, thus increasing the confidence level of the methodology as a guideline for designing good handling qualities as well as for their assessment.

The landing task is normally identified as compensatory but, unlike tracking, is essentially a low-gain task with the pilot's control activity centered around a fixed-phase lag value of about 120 deg (Ref. 3). The analysis of the landing task is based on the LATHOS experiment data base relative to class IV, category C aircraft[1] and involves both instrument landing as well as visual landing tasks. In all, 16 configurations were analyzed with different roll time constant τ_r, pure time delay τ_d, and roll control effectiveness. A detailed description of the configurations can be found in Ref. 4. The roll metrics defined for this analysis[2] are the effective time delay τ_{eff} (system delay in response to a change in forcing function as seen by the pilot), roll control effectiveness $L'_{F_{as}} = p_{ss}/\tau_r$, and acceleration ratio R_a defined as the ratio between maximum and initial roll accelerations and given by $R_a = \ddot{\phi}_{\max}/(L_{F_{as}})$.

The next two sections present the results of the analysis, level 1 boundaries are identified as well as pilot-induced oscillations (PIO) and ratcheting-prone configurations using the roll metrics just described.

Time Response Analysis

Gibson's method is not directly applicable in the time response analysis because of the first-order nature of the behavior in roll as shown in Eq. (1):

$$\frac{p}{F_{as}} = \frac{\tau_r L'_{F_{as}}}{(\tau_r s + 1)} \tag{1}$$

The metrics described in the previous section, however, can be effectively used to separate regions with good response from regions presenting PIO and other undesirable oscillations. The results are summarized in Fig. 1, where roll control effectiveness $L'_{F_{as}}$ and effective time delay τ_{eff} are plotted against each other. Large time delays are usually associated with sluggish response and possibly PIO as shown by configurations M and E.

The roll control effectiveness also represents the initial roll acceleration to a step command (computed from the initial value theorem applied to the acceleration transfer function), and its minimum value is independent of the delay, whereas the upper bound is affected by it as shown in the figure and reported in the pilot comments.

Too high values of initial acceleration are unacceptable, and the results in Fig. 1 are consistent with the limits given in the present military specification.[5] On the other hand, lower values of roll acceleration are acceptable unless the time delay is too large. For the landing task, the following boundaries can be identified.

Level 1: $10 < L'_{F_{as}} < 42\ \text{s}^{-2}/\text{lb}$, $\tau_{\text{eff}} < 0.11$ s

Level 2: $L'_{F_{as}} < 10$ and $42 < L'_{F_{as}}\ \text{s}^{-2}/\text{lb}$, $\tau_{\text{eff}} < 0.15$ s

Separate comments must be made for configuration G. There appears to be a discrepancy between its location well within level 1 boundaries, and the pilot comments indicating the presence of ratcheting and a level 2 rating. In this case, the acceleration ratio R_a can be used effectively to identify the anomaly. It can be observed that normal response (absence of oscillations and instabilities) requires the acceleration ratio to be $0.76 < R_a < 0.94$. Lower values are indicative of ratcheting, whereas values of R_a near unity imply the presence of PIO. Since configuration G has $R_a = 0.75$, the ratcheting instability can be accounted for in Fig. 1. In conclusion, boundaries of levels 1 and 2 can be identified, keeping in mind the constraints on R_a.

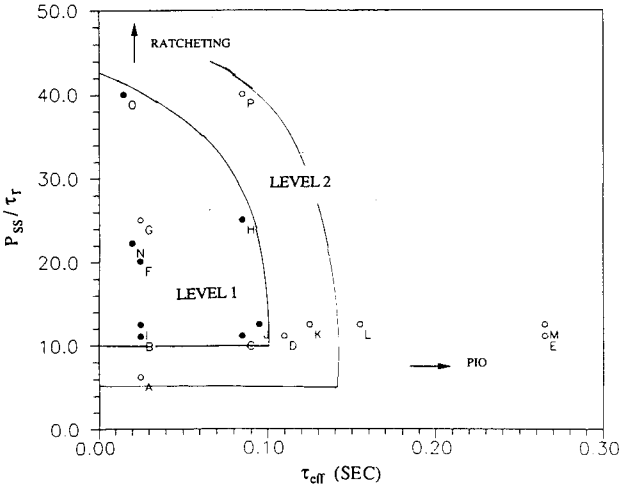

Fig. 1 Time response analysis results.

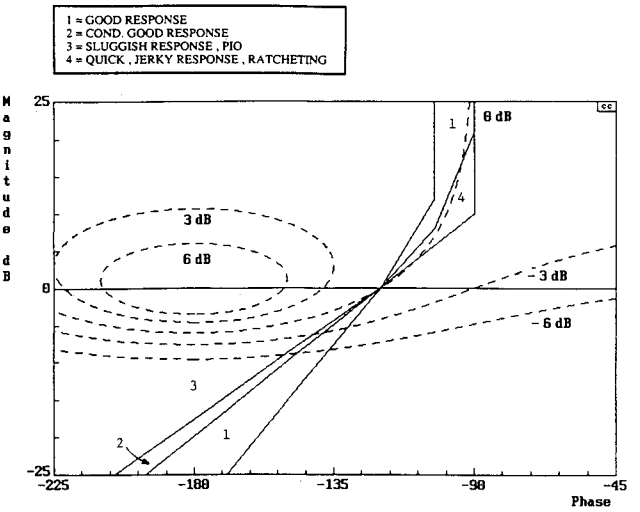

Fig. 2 Frequency response boundaries.

Received Sept. 10, 1990; revision received July 2, 1991; accepted for publication July 19, 1991.

*Graduate Student, Department of Aerospace Engineering.
†Associate Professor, Department of Aerospace Engineering. Senior Member AIAA.

Frequency Response Analysis

The frequency response analysis is helpful in identifying problems associated with closed-loop instabilities like pilot-induced oscillations and ratcheting. The landing frequency analysis is carried out in a fashion similar to the Gibson's frequency analysis done for the longitudinal landing case.[2,3] The frequency response for the longitudinal landing task looks at the open-loop response of the pitch attitude. The attitude gain is adjusted so as to have a unity gain with a phase lag value of 120 deg. Similarly, the bank angle frequency response with the loop gain adjusted so as to have a unity gain at a 120-deg phase lag value is considered in the present analysis. Using pilot comments,[1] we obtain the frequency response boundaries for the task as shown in Fig. 2. Comparison with the results in Ref. 2 clearly shows the difference in boundaries between tracking and landing tasks.

The various regions labeled on Fig. 2 correspond to different aircraft responses. Four main zones are identified: 1) optimal approach and landing region, 2) conditionally good region, 3) sluggish, PIO prone region, and 4) quick, oscillatory, and ratcheting-prone region.

The region marked 1 shows a zone of good and optimal behavior; configurations B, I, and J, for example, all satisfy these boundaries. Pilot-induced oscillations are excited when the crossover frequency ω_{180} is low (typically $\omega_{180} < 0.5$ Hz) and the phase lag increases rapidly with little or no gain attenuation. Regions 2 and 3 are representative of the PIO and sluggish response, mainly due to the effect of large time delays. This region is divided into a sluggish PIO prone section 3 and a conditionally good response section 2. The condition for the response to be good is that ω_{180} be greater than 0.5 Hz. For example, configuration C lies in this region and has $\omega_{180} > 0.5$ Hz and it is commented to have good flying qualities, whereas configuration L has $\omega_{180} < 0.5$ Hz and exhibits PIO. Configurations lying in region 3 have sluggish or delayed response. Pilot-induced oscillations are also seen to accompany these responses provided the condition of $\omega_{180} < 0.5$ Hz is satisfied. Region 4 includes configurations exhibiting sharp, quick, oscillatory responses as well as ratcheting. Note that the presence of the ratcheting instability requires a crossover frequency ω_{180} between 12 and 18 rad/s and a magnitude greater than zero dB in the roll acceleration frequency response, a condition similar to what was found for the roll tracking task.[2] In summary, Fig. 2 shows the general trend relating roll instabilities to phase rate and magnitude attenuation.

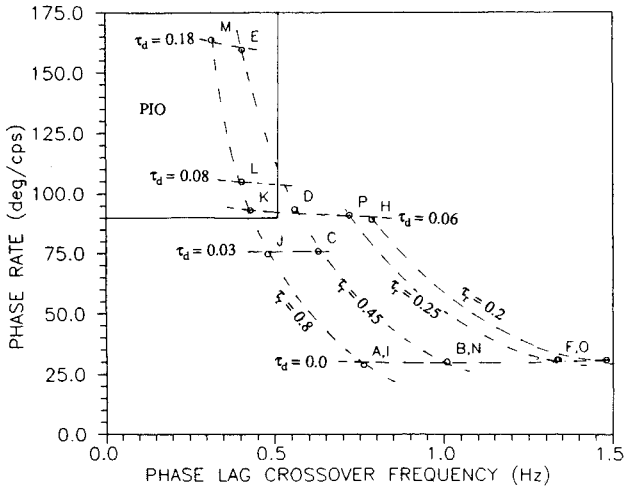

Fig. 3 Phase rate boundary.

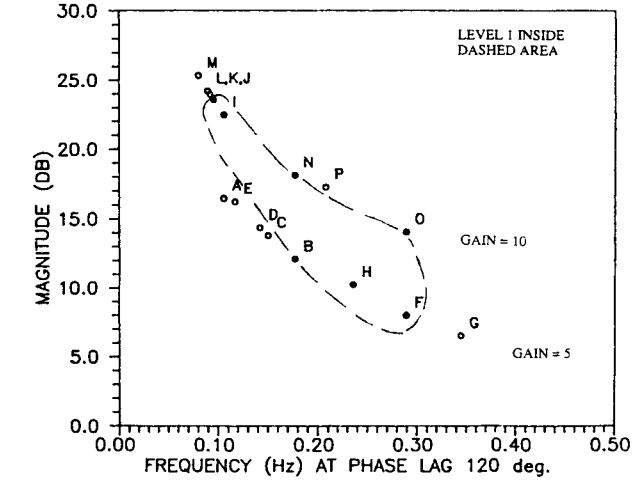

Fig. 4 Control sensitivity boundary for level 1 (thumbprint).

Table 1 Frequency response results

Deficiency	Usage
PIO	$\omega_{180} < 0.5$ Hz and $P_r \geq 90$ deg cps or $\tau_r \leq 0.3$ s
Ratcheting	12 rad/s $\leq \omega_{180} \leq$ 18 rad/s acceleration > 0 db

Frequency boundaries plots, however, do not show the separate effects of control sensitivity or τ_r or time delay τ_d directly. Variations in roll time constant and time delay on dynamic instabilities are shown in Fig. 3 by plotting phase rate vs phase lag crossover frequency. The figure shows τ_r and τ_d isoclines, where constant τ_r are represented by vertical curves moving to the left as τ_r increases, and constant τ_d are the horizontal curves that shift upwards as τ_d increases. From Fig. 3 it is clear how small values of τ_r may affect ratcheting (below MIL-STD boundary of 0.3 s). Time delay τ_d, on the other hand, affects phase rate that in turn is indicative of PIO. Since phase rate P_r increases with τ_d, large phase rate values cause PIO, and the horizontal boundary drawn for $P_r = 90$ deg/cps separates PIO and non-PIO regions.

To account for sensitivity effects, a thumbprint plot is drawn in Fig. 4. The ordinate of the thumbprint is the gain equalization required to attain a phase lag crossover of 120 deg, whereas the abscissa represents the corresponding frequency at the crossover point. The central zone identifies a possible level 1 region. The frequency response analysis results are summarized in Table 1, which shows ranges of the metrics leading to instability.

Conclusions

The Note has presented a validation of Gibson's method when applied to the analysis of highly augmented aircraft lateral handling qualities, and new boundaries for satisfactory dynamic behavior have been developed for the landing task. The results confirm the validity of the methodology as a general design tool for good handling qualities when the aircraft behavior possesses considerable high-order effects.

References

[1]Monagan, S. J., "Lateral Flying Qualities of Highly Augmented Fighter Aircraft," AFWAL-TR-81-3171, Vol. 1, Air Force Wright Aeronautical Lab., Wright-Patterson AFB, OH, June 1982.

[2]Innocenti, M., and Thukral, A., "Roll Performance Criteria for Highly Augmented Aircraft," *Journal of Guidance, Control and Dynamics*, Vol. 14, No. 6, 1991, pp. 1277-1286.

[3]Gibson, J. C., "Piloted Handling Qualities Design Criteria for High Order Flight Control Systems," AGARD-CP-333, April 1982.

[4]Thukral, A. "Criteria for Lateral Handling Qualities Evaluation," M.S. Thesis, Dept. of Aerospace Engineering, Auburn Univ., AL, June 1991.

[5]Anon., "Military Standard Flying Qualities of Piloted Vehicles," MIL-STD-1797, March 1987.